# Segregation and Dispersion of a Binary System of Particles in a Fluidized Bed

**K. P. Galvin and R. Swann**
School of Engineering, University of Newcastle, Callaghan, NSW 2308, Australia

**W. F. Ramirez**
Dept. of Chemical Engineering, University of Colorado, Boulder, CO 80309

*DOI 10.1002/aic.10957*
*Published online August 24, 2006 in Wiley InterScience (www.interscience.wiley.com).*

*The steady-state segregation and dispersion of a binary system of particles in a liquid-fluidized bed was investigated. One of the species had a density of 1,600 kg/m$^3$ and the other 1,900 kg/m$^3$, and both exhibited a narrow size range of 1.00 to 1.18 mm. A generalized model for describing the dispersion coefficient,* D*, was proposed. That is,* $D = \alpha d U_f/\phi$*, where* d *is the particle diameter,* $U_f$ *the local interstitial fluid velocity, and* $\phi$ *the local volume fraction of solids. The model had one adjustable parameter* $\alpha$*, which was fixed at 0.7 for both particle species and for the six different superficial fluidization velocities used. The particle segregation was described with reference to the monocomponent fluidization parameters of the two species, based on the Richardson and Zaki equation. Good descriptions of the concentration profiles of the two species were produced for all superficial velocities examined. Additional experiments involving other binary systems were also conducted in order to test the generality of the model. These systems involved particles of closer settling velocities, and, hence, displayed more mixing. Very small adjustments in the terminal velocities of the species, typically 2%, were needed to achieve satisfactory agreement between the theoretical and experimental concentration profiles, with the model parameter,* $\alpha$*, equal to 0.7. This adjustment was justified because of apparent changes in the average particle sizes of the two species due to particle-size segregation.*  *AIChE J,* 52: 3401–3410, 2006
*Keywords: fluidization; binary; dispersion; segregation; slip velocity; granular temperature; liquid fluidized*

## Introduction

The steady-state distribution of a binary system of particles in a liquid-fluidized bed operated under batch conditions was investigated. In a binary particle system there is a tendency for each particle species to segregate, and, hence, form a monocomponent zone, with the zone of higher-bulk density residing below.[1] Between the two-monocomponent zones there exists a transition containing the two species, with the particles distributed according to the balance that develops between the particle segregation and dispersion. In describing the dispersion in fluidized beds, the dispersion coefficient is generally treated as an adjustable parameter, given that there is no reliable way to predict it. For example, Batchelor[2] proposed that $D = \alpha' aU$, where $a$ is the particle radius, $U$ the superficial-fluid velocity, and $\alpha'$ a value between 0.5 and 5. Davis and Hassan[3] indicate $\alpha'$ increases from about 8 to 12 as the volume fraction decreases from 0.15 to 0.05.

The primary variable in this study was the superficial fluidization velocity $U$, which was varied over a range that was

Correspondence concerning this article should be addressed to K. Galvin at kevin.galvin@newcastle.edu.au.

significant relative to the particle terminal velocities. A full understanding of the functional dependence of the dispersion coefficient $D$, on the operating conditions should permit a complete description of the concentration profiles at any fluidization velocity. In previous studies, the effect of the fluidization velocity on the dispersion coefficient has usually been expressed in terms of simple scaling laws[4-6] of the form, $D \sim U^{\beta}$.

It is worth considering the approach taken based on the kinetic theory of gases to obtain an expression for the dispersion coefficient.[7] We use here a simpler analysis to arrive at an approximate result. The principal length scale in the problem is the mean free path, which is the expected distance a particle must travel before there is a collision with another particle. Particles with centers located beyond a distance $d/2$, from the surface of our moving particle do not collide with our particle. Hence, in order to examine the potential for a collision, we need to determine the number of particles within the relevant volume, defined by a tube of length $L$ and diameter $2d$. In a fluidized bed containing particles of diameter $d$, the volume fraction of solids is $\phi = N(\pi/6)d^3$, where $N$ is the number of particles per unit volume of the bed. Thus, the number of particles n, within the relevant volume is, $n = (\pi/4)(2d)^2LN = 6\phi L/d$. Thus, the mean free path is $L/n = d/(6\phi)$. Assuming the average particle-velocity scales directly with the interstitial fluid velocity $U_f$, the dispersion coefficient should be proportional to $dU_f/\phi$.

Thus, we propose that the dispersion coefficient varies as, $D = \alpha dU_f/\phi$, where $\alpha$ is a constant, $d$ the particle diameter, $U_f$ the interstitial-fluid velocity, and $\phi$ the volume fraction of solids. In order to apply this general relationship, it is necessary to permit the dispersion coefficient to vary throughout the fluidized bed according to local changes in the interstitial fluid velocity, and the volume fraction of solids. We are not aware of any previous study that has involved the application of a local dispersion coefficient, which varies in this way. As already noted, the usual approach is to assign a single value for the dispersion coefficient to a given particle species, usually on the basis of a least squares fit of the theoretical concentration profile to the experimental concentration profile.

A further focus of this study was on a binary system of particles of similar size, with the key difference between each of the two-particle species being the particle density. Thus, in principle, the dispersion coefficient for the two-particle species used in this study should be the same. Given this is the first study of its kind to use a binary system of species that differ only by way of the particle density, there is an opportunity to examine whether the particle density influences the dispersion coefficient, in which case there would be a different value of the unknown constant $\alpha$, for each particle species.

## Theory

In this analysis, the upward direction is taken as positive. Hence, given that all particles are denser than the fluid, the slip velocity of a particle is always a negative value. However, the terminal velocity of a particle is treated as a positive scalar, with a minus sign used with the terminal velocity to produce a negative value. Species $i$ is assumed to be the faster settling species, and, hence, establishes its monocomponent zone at the base of the vessel, with species $j$ located above. Although we describe the model in terms of the species $i$, the subscript $i$, can be changed to $j$ to obtain the corresponding relationship for species $j$. Final expressions are given, however, for both species $i$ and $j$.

Within the monocomponent zone of species $i$, the downward slip velocity $U_{si}$, of the particles is equal in magnitude to the upward interstitial fluid velocity $U_f$, and, hence, the segregation velocity

$$U_i = U_{si} + U_f \tag{1}$$

is zero. Here, there is also no concentration gradient, and, hence, no dispersion. However, for a particle of species $i$ located outside its monocomponent zone, a nonzero segregation velocity arises, with a direction appropriate for returning the particle to its monocomponent zone. Thus, the segregation velocity for the faster settling species will be in the downward direction (negative value), while for the slower settling species will be upward (positive value).

The segregation velocities are responsible for driving the system of particles toward a final equilibrium state, consisting of two monocomponent zones separated by a transition zone. Within the transition zone, each species exhibits a segregation flux dependent on the product of the local segregation velocity $U_i$, and local species-volume fraction, $\phi_i$. The faster settling species are constantly driven downward, and the slower settling species upward. This tendency to segregate, however, is opposed by a dispersive flux for each species, which depends on the local product of the concentration gradient, $d\phi_i/dz$, and dispersion coefficient $D_i$, where $\phi_i$ is the volume fraction of species $i$, and $z$ the distance above the base of the vessel.

According to Kennedy and Bretton[8], the balance between the dispersive and segregation fluxes of each species is given universally by

$$D_i \frac{d\phi_i}{dz} = U_i \phi_i \tag{2}$$

Asif and Petersen[6] proposed a relationship of the following form for the segregation velocity of species $i$. That is

$$U_i = U_{mi}\left(1 - \frac{\phi_i}{\phi_{mi}}\right) = U_{mi}(1 - \phi_{ni}) \tag{3}$$

where $U_{mi}$ is the maximum possible segregation velocity of species $i$, which occurs when one particle of species $i$ is immersed within the monocomponent zone of the other species $j$. In Eq. 3, $\phi_i$ is the local volume fraction of species $i$, $\phi_{mi}$ the monocomponent concentration of species $i$, and $\phi_{ni} = \phi_i/\phi_{mi}$ the normalized concentration of species $i$. Equation 3 is clearly just a proposition, as it has not been derived. However, the equation has an analytical appeal, given that when $\phi_{\mathrm{ni}} = 0$ there is effectively a single particle of species $i$ in the monocomponent zone of species $j$, and, hence, the maximum segregation velocity is obtained. Conversely, when $\phi_{ni} = 1$, the particle of species $i$ is in the monocomponent zone of species $i$, and, hence, the segregation velocity is zero. Equation 3 also assists in obtaining a direct analytical solution to the Kennedy and Bretton[8] equation.

Consider a single particle of species $i$ immersed within the monocomponent zone of species $j$. According to the Locket and Al-Habooby[9] model for the particle-slip velocity,

$$U_{si} = -U_{ti}(1 - \phi_{mj})^{n_i - 1} \tag{4}$$

where $U_{ti}$ is the magnitude of the terminal velocity of species $i$, and $n_i$ is an exponent. The interstitial fluid velocity in the monocomponent zone of species $j$ is

$$U_f = \frac{U}{(1 - \phi_{mj})} = U_{tj}(1 - \phi_{mj})^{n_j - 1} \tag{5}$$

The maximum segregation velocity of species $i$ occurs when species $i$ has a volume fraction of solids of zero, and species $j$ has a volume fraction of solids equal to its monocomponent value. Combining the description for the slip velocity of species $i$ under this condition with the interstitial fluid velocity $U_f$, under this condition allows the value of $U_i$ to be obtained under this extreme condition. This value of $U_i$ is referred to as the maximum segregation velocity $U_{mi}$, and is obtained by combining Eqs. 1, 4, and 5 and then setting $U_i = U_{mi}$. That is

$$\begin{aligned} U_{mi} &= -U_{ti}(1 - \phi_{mj})^{n_i - 1} + U_{tj}(1 - \phi_{mj})^{n_j - 1} \\ &= (U_{tj} - U_{ti})(1 - \phi_{mj})^{n-1} \end{aligned} \tag{6}$$

where it is assumed the exponent $n_i = n_j = n$. Asif and Petersen[6] treated the value of $U_{mi}$ as a constant for a system operated at a fixed superficial velocity $U$. Combining Eqs. 3 and 5 with Eq. 6 gives the segregation velocity of component $i$ under all conditions. That is

$$U_i = (1 - \phi_{ni})\left(1 - \frac{U_{ti}}{U_{tj}}\right)U_f = (1 - \phi_{ni})U_{ij}U_f \tag{7}$$

where the normalized segregation parameter $U_{ij}$, is

$$U_{ij} = \left(1 - \frac{U_{ti}}{U_{tj}}\right) \tag{8}$$

Equation 7 is equivalent to that used by Asif and Petersen[6], provided the interstitial-fluid velocity corresponds to the level that exists in the monocomponent zone of component $j$. However, in this article we have chosen to permit the interstitial-fluid velocity to adopt the value of the local interstitial-fluid velocity, rather than the specific value used in the derivation (that is, the interstitial-fluid velocity that arises in the monocomponent zone of component $j$). This subtle change has a negligible effect on the variation in the segregation velocity with volume fraction, given that the segregation velocity still decreases from the same extreme value of $U_{mi}$ in the monocomponent zone of species $j$ toward the same level of 0 in the monocomponent zone of species $i$. Given Eq. 3 is empirical in its origin, and not based on any rigorous validation, Eq. 7 is no more or no less correct. Nevertheless, we argue that Eq. 7 is a better representation, given that it effectively uses the total-volume fraction of solids at a given location to determine the maximum segregation velocity of a given species.

The empirical expression proposed in this study to describe the dispersion coefficient is

$$D_i = \frac{\alpha d_i U_f}{\phi_i + \phi_j} \tag{9}$$

where $\alpha$ is a constant, and $d_i$ the particle diameter. If Eq. 9 is reasonable, then it should be possible to describe the segregation and dispersion of the binary system with one value for the constant, $\alpha$, over a broad range of fluidization velocities.

Substituting Eqs. 7 and 9 into Eq. 2, and rearranging gives

$$\frac{d\phi_i}{(\phi_i + \phi_j)\phi_i(1 - \phi_{ni})} = \frac{U_{ij}dz}{\alpha d_i} \tag{10}$$

In order to solve Eq.10, it is desirable to eliminate the variable $\phi_j$. Asif and Petersen[6] has suggested the following identity

$$\phi_{ni} + \phi_{nj} = 1 \tag{11}$$

There is no fundamental reason why the system should adhere rigorously to Eq. 11, however, the equation does provide a convenient and relatively accurate basis for removing the variable $\phi_j$ from Eq. 10. Indeed, the experimental data are consistent with Eq. 11, especially in the zone between the two monocomponent zones, where the relationship is needed. It is noted that this identity is not used generally to solve this problem, only to estimate the total-volume fraction of the solids in Eq. 9. Normalizing the volume fraction terms in Eq. 10, and using Eq. 11 to eliminate $\phi_j$ from Eq. 10, gives

$$\frac{d\phi_{ni}}{[\phi_{ni}(\phi_{mi} - \phi_{mj}) + \phi_{mj}]\phi_{ni}(1 - \phi_{ni})} = \frac{U_{ij}dz}{\alpha d_i} \tag{12}$$

It follows that

$$\frac{d\phi_{ni}}{(\phi_{ni} + \beta_i)\phi_{ni}(1 - \phi_{ni})} = \frac{(\phi_{mi} - \phi_{mj})U_{ij}dz}{\alpha d_i} \tag{13}$$

where

$$\beta_i = \frac{\phi_{mj}}{(\phi_{mi} - \phi_{mj})} \tag{14}$$

Hence

$$-\frac{d\phi_{ni}}{(1 + \beta_i)(\phi_{ni} + \beta_i)} + \frac{d\phi_{ni}}{\phi_{ni}} + \frac{\beta_i d\phi_{ni}}{(1 + \beta_i)(1 - \phi_{ni})} = \frac{\phi_{mj}U_{ij}dz}{\alpha d_i} \tag{15}$$

Integration of Eq, 15 from $\phi_{ni} = \phi_{nio}$ to $\phi_{ni}$, and $z = h$ *to* $z = z$, gives

$$-\frac{1}{(1+\beta_i)}\ln\left(\frac{\phi_{nio}+\beta_i}{\phi_{ni}+\beta_i}\right)+\ln\phi_{nio}-\ln\phi_{ni}+\frac{\beta_i}{(1+\beta_i)}\ln\left(\frac{1-\phi_{ni}}{1-\phi_{nio}}\right)=\frac{\phi_{mj}U_{ij}(z-h)}{\alpha d_i} \quad (16)$$

where $h$ is the height of the fluidized bed. Noting that in general, $\phi_{nio} \ll 1$, it follows that

$$\left(\frac{\phi_{ni}}{\beta_i}+1\right)^{[1/(1+\beta_i)]}\left(\frac{(1-\phi_{ni})^{[\beta_i/(1+\beta_i)]}}{\phi_{ni}}\right)=\exp(\omega_i-\kappa_i(h-z)) \quad (17)$$

where

$$\omega_i=-\ln(\phi_{nio}) \quad (18)$$

and

$$\kappa_i=\frac{\phi_{mj}U_{ij}}{\alpha d_i} \quad (19)$$

Equation 17 is readily solved by specifying the value of $\phi_{ni}$, and then computing the corresponding distance z. The adjustable parameters in Eq. 17 are $\omega_i$ and $\kappa_i$. The value of $\kappa_i$ governs the value of the dispersion coefficient, while $\omega_i$ in conjunction with $\kappa_i$ governs the volume of the species $i$ per unit of vessel area. Thus, given that the inventory of solids is a known experimental quantity, there is just one adjustable parameter $\kappa_i$, which in turn provides the value of the unknown quantity $\alpha$.

The corresponding solution for the second species $j$ is obtained using

$$-\frac{d\phi_j}{(1+\beta_j)(\phi_{nj}+\beta_j)}+\frac{d\phi_{nj}}{\phi_{nj}}+\frac{\beta_j d\phi_{nj}}{(1+\beta_j)(1-\phi_{nj})}=\frac{\phi_{mi}U_{ji}dz}{\alpha d_j} \quad (20)$$

where

$$\beta_j=\frac{\phi_{mi}}{(\phi_{mj}-\phi_{mi})} \quad (21)$$

and

$$U_{ji}=\left(1-\frac{U_{tj}}{U_{ti}}\right) \quad (22)$$

In this case the integration proceeds from $\phi_{nj}=\phi_{njo}$ to $\phi_{nj}$ and from $z = 0$ *to* $z = z$. That is

$$\left(\frac{\phi_{nj}}{\beta_j}+1\right)^{[1/(1+\beta_j)]}\left(\frac{(1-\phi_{nj})^{[\beta_j/(1+\beta_j)]}}{\phi_{nj}}\right)=\exp(\omega_j-\kappa_j z) \quad (23)$$

where

$$\omega_j=-\ln(\phi_{njo}) \quad (24)$$

and

$$\kappa_j=\frac{\phi_{mi}U_{ji}}{\alpha d_j} \quad (25)$$

## Experimental

A Perspex tube, 50 mm in dia., and 2,000 mm high, was used to conduct the fluidization experiments. Fluidization water was supplied from a head tank to the base of the vessel via a distributor plate containing 127 evenly spaced 1 mm diameter holes. A carefully calibrated rotameter was used to measure the water rate. Superficial fluidization velocities were also confirmed using a "bucket and stopwatch" once equilibrium was reached. Glass beads filled the fluidization chamber in order to ensure an even flow passing up through the distributor plate. Sampling valves were typically located every 70 mm along the vessel wall. At the same elevations, pressure tappings were also installed. Great care was taken to ensure the vessel was vertical, as a slight inclination caused complex flow patterns, and, hence, a significant disruption to the transition zone.

The particles used in the study were supplied by Partition Enterprises. The two species had contrasting colors, which was useful in visually observing the distribution of the particles, and in separating samples of the two species. One of the particle species had a density of 1,600 kg/m$^3$, and the other a density of 1,900 kg/m$^3$. Each consisted of particles in the narrow-size range 1.00 to 1.18 mm. While it would have been preferable for all of the particles to be the same size, the density difference chosen was sufficient for this system to segregate almost entirely on the basis of a difference in density. Of course, with a much smaller density difference, the observed mixing in the transition zone would be influenced by segregation on the basis of the particle size.

Experimentally, the objective was to measure accurately the volume fraction of each particle species at each sampling elevation down the vessel. We have previously measured the proportions of solid and water, together with the pressure gradient, and generally obtained reasonable data.[10,11] However, where the volume fraction of a species is close to zero, the sampling errors can sometimes lead to slightly negative volume fraction values. The negative values arise when the solid and water masses are combined with the pressure gradient data. These errors presumably occur because the exact proportions of water and solid particles can be influenced by a very small degree of filtration as the suspension flows through the sampling valve. However, it is possible to sample the particle composition accurately given that the two species will behave in the same way during the discharge. So, our approach was to discharge a relatively small sample through each valve, from the top position downward. The water content of the samples was not considered. The particles were then hand separated into the two-density species, on the basis of color, and weighed to obtain the mass and, hence, volume ratios of the species. Typically, several thousand particles were separated in each sample.

## Analysis of Experimental Data

The pressure tappings down the vessel wall were connected via a manifold to a pressure transducer, and pressure readings taken in order to obtain the density of the suspension at a given location. The value of the suspension density at a given level was calculated using the pressure gradient obtained at the sampling levels in question using adjacent pressure tapping values. Given the tubes connected to the transducer were filled with water, and water was the fluidizing fluid, the suspension density, $\rho_{susp}$, was related to the measured pressure drop, $\Delta P$, by

$$\Delta P = (\rho_{susp} - \rho_f)\, g \Delta z \tag{26}$$

where $\rho_f$ is the density of water, $g$ the acceleration due to gravity, and $\Delta z$ the distance between the two tappings. The suspension density can also be related to the volume fractions, $\phi_i$ and $\phi_j$, of the two-solid species, and $\phi_f = 1 - \phi_i - \phi_j$ of the fluid. That is

$$\rho_{susp} = \phi_i \rho_i + \phi_j \rho_j + (1 - \phi_i - \phi_j)\rho_f \tag{27}$$

where $\rho_i$, $\rho_j$, and $\rho_f$ are the densities of the two-particle species and the fluid, respectively. The concentration ratio, $f = \phi_i/\phi_j$ of the two species is readily and accurately obtained from a small sample of the suspension, where $m_i$ and $m_j$ are the masses of the two species in the sample. That is

$$f = \left(\frac{m_i}{\rho_i}\right) \Big/ \left(\frac{m_j}{\rho_j}\right) \tag{28}$$

By combining the earlier equations, an expression is then obtained for the volume fraction of the second species, which combined with the value of $f$ yields the volume fraction of the first species. That is

$$\phi_j = \frac{\rho_{susp} - \rho_f}{f(\rho_i - \rho_f) + (\rho_j - \rho_f)} \tag{29}$$

This approach is far more robust than one reliant on samples that are meant to contain the correct proportion of the fluid.

A careful assessment of the procedure described earlier indicates that the adopted method is sufficiently accurate for the purposes of this study. This assessment was conducted because of concerns that the distance of 70 mm between the pressure tappings may prove to be too great, relative to the heights of the transition zones. The assessment involved a simulation of the experimental study, commencing with a numerical representation of the concentration profiles. It was then assumed that these were the true concentration profiles. Pressure gradients, determined using only the information at each of the pressure tapping heights were then obtained, and exact concentration ratios were obtained at each of the sampling positions. These concentration ratios were then combined with the simulated pressure gradient information to obtain the simulated experimental volume fractions of the two species. These data were then compared with the "true values" so as to evaluate the accuracy of the experimental method.

**Table 1. Species Parameter Values for the Richardson and Zaki Equation**

| Particle Species (kg/m$^3$) | Terminal Velocity $U_{ti}$ (m/s) | Exponent Value $n_i$ |
|---|---|---|
| 1600 | 0.0699 | 3.1 |
| 1900 | 0.0837 | 3.1 |
| 1300 | 0.046 | 3.2 |
| 1400 | 0.052 | 3.2 |
| 1700 | 0.080 | 3.1 |
| 1800 | 0.085 | 3.1 |

In general the accuracy of the method was found to be high, thus, indicating that the spacing of 70 mm was adequate. However, depending on the position of the transition zone relative to the sampling points, one of the data points was sometimes inaccurate. The inaccurate data point always involved the lower-density species. The inaccuracy, when it occurred, was also obvious, given the concentration value was always higher than the monocomponent value at a position that should have a concentration perhaps 20% below the monocomponent value. Examination of the data from this article suggests that there were no significant errors of the kind described. Even if there were such errors, it would be straightforward to identify the discrepancy. It is also argued that the main merit of the data presented in this study is in the way the whole system behaves as the superficial velocity increases, which is certainly captured by the overall set of experimental results.

The monocomponent expansion data were summarized by the parameters in the Richardson and Zaki equation[12]. That is

$$U = U_{ti}(1 - \phi_i)^{n_i} \tag{30}$$

where $U$ is the superficial fluidization velocity, $U_{ti}$ the terminal velocity of the species, $\phi_i$ the volume fraction of the solids, and $n_i$ the value of the exponent. A common exponent for the two species was obtained. The values of the parameters are summarized in Table 1 for the two species.

Binary fluidization experiments were then conducted using 0.139 kg of the 1600 kg/m$^3$ particles and 0.169 kg of the 1,900 kg/m$^3$ particles, with the system permitted to achieve equilibrium over a period of 30 min at a specific fluidization velocity. Separate experiments were run using superficial velocities ranging from 0.031 to 0.058 m/s.

## Results and Discussion

Concentration profiles for the two particles species of density 1,600 kg/m$^3$ and 1,900 kg/m$^3$, obtained using six different fluidization velocities, are reported in Figures 1a, b, c, d, e and f. A monocomponent zone of the 1,900 kg/m$^3$ species forms at the base. The concentration decreases through the transition zone to zero, while the concentration of the 1,600 kg/m$^3$ species rises through the transition zone to form a monocomponent zone. It is also evident that in a number of cases there is a drop-off in the concentration of the less dense species toward the top of the bed. This behavior has been observed previously by Ramirez and Galvin[11], and may be a consequence of the fact that the system is close, but not quite at steady state, or a consequence of the particle-size distribution.[13,14]

The curves shown through the data were generated using

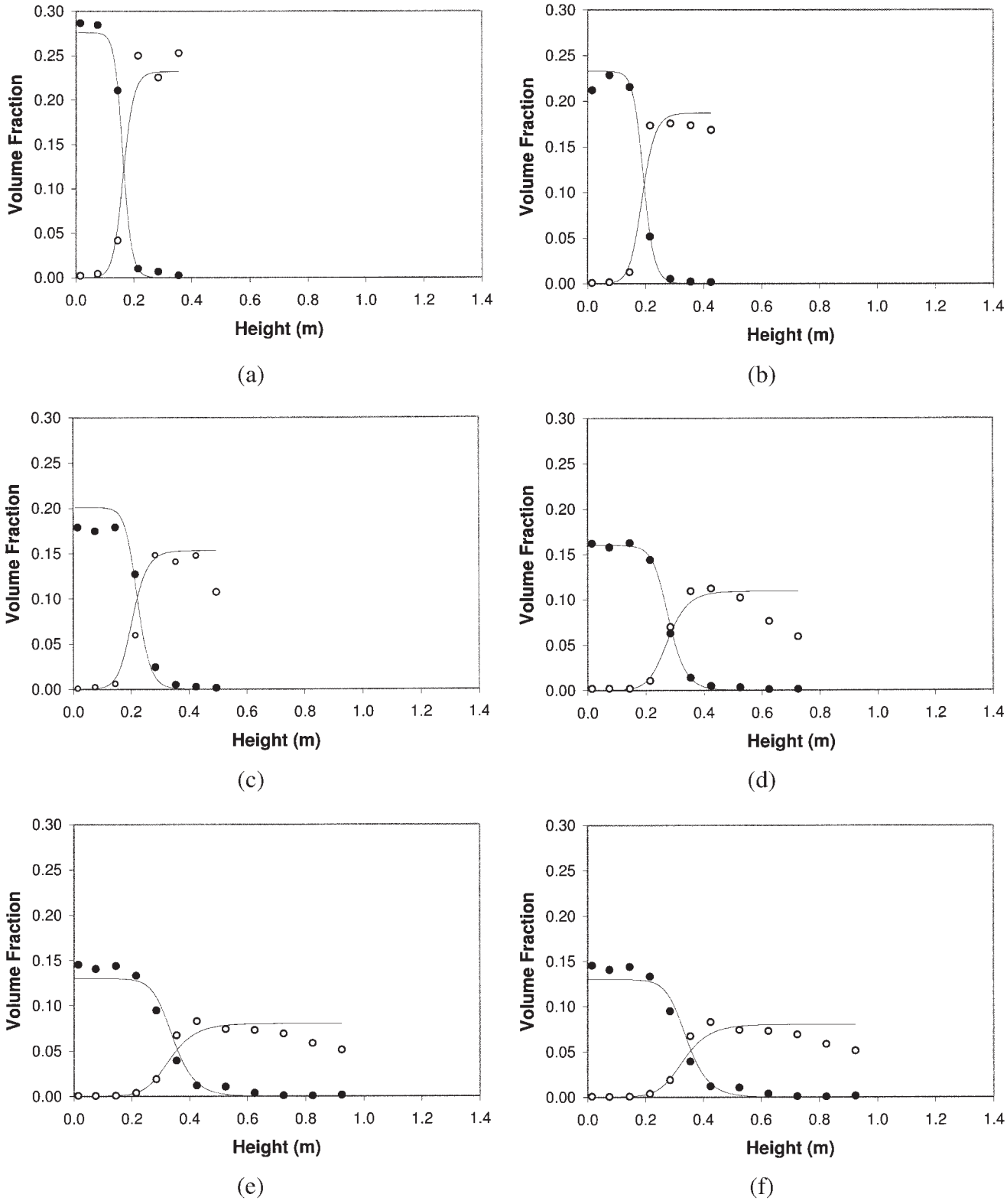


**Figure 1. Influence of the fluidization velocity on the concentration profile of particle species having densities of 1,600 and 1,900 kg/m$^3$.**

The open symbols and closed symbols denote the low and the high-density species, respectively. Six cases are shown ranging from low-to high-superficial velocities ((a) 0.031 m/s; (b)0.037 m/s; (c) 0.042 m/s; (d) 0.049 m/s; (e) 0.054 m/s; and (f) 0.058 m/s). The curves through the data are based on Eqs. 17 and 23, with the dispersion coefficient based on $\alpha = 0.7$ and $d = 0.00109$ m. Other parameter values, such as the monocomponent concentrations and segregation parameter values are derived from Table 1.

Eqs. 17 and 23. The monocomponent-volume fractions were calculated using the Richardson and Zaki[12] equation together with the monocomponent parameter values listed in Table 1. The normalized segregation parameters $U_{ij}$ and $U_{ji}$, were also obtained from the data in Table 1. The total specific volume of species $i$ used in the experiments (total volume of particles of species $i$ relative to the vessel area) was $V_{io} = 0.045$ m$^3$/m$^2$, and the total for species $j$ was $V_{jo} = 0.044$ m$^3$/m$^2$. Thus, the value of $\phi_{nio}$, and the fluidization-bed height $h$, in Eq. 17 were set in order to ensure the area under the concentration profile curve for species $i$ was equal to $V_{io} = 0.045$ m$^3$/m$^2$. The value of $\phi_{njo}$ in Eq. 23 was set using the same approach, the aim being to ensure the area under the curve for species $j$ was equal to $V_{jo} = 0.044$ m$^3$/m$^2$. The identity proposed by Asif and Petersen[6] could also be used to couple the descriptions for the two species, and in turn assist with calculating a value for $\phi_{njo}$.

In Figures 1d, e and f, however, the specific volume of species $j$ was set equal to values of 0.0485, 0.047 and 0.055, respectively. These values are higher than the experimental values. The increase was introduced to counter the drop-off in the concentration of species $j$ at the very top of the fluidized bed. The excess volume used is easily calculated by comparing the theoretical monocomponent curve, and the experimental data at the top of the bed. This correction only impacted on the value of the integration constant $\phi_{njo}$, and had no impact on the required value of $\alpha$, and, hence, the expression for the dispersion coefficient.

Remarkably, a single expression for the dispersion coefficient, with $\alpha = 0.7$, was sufficient to describe the concentration profiles of both species, at all fluidization velocities. Given the volumes of the two-particle species used in the experiments were known, the area under each of the concentration profile curves was also known. The monocomponent fluidization parameters were also known, and, hence, the monocomponent concentrations of each species could be calculated for any superficial-fluidization velocity. Hence, if we now consider $\alpha = 0.7$ to be a fixed constant, we have succeeded in describing the segregation and dispersion of these two-particle species over a broad range of fluidization velocities, with no other adjustable parameters. Other binary systems are considered later in this article to explore further the generality of the expression for the dispersion coefficient proposed in this article.

The two-particle species so far examined were selected for this study, because the thickness of the transition zone was generally large enough to be measured and small enough to ensure there would be monocomponent zones either side. It is interesting to consider why the thickness of the transition zone is negligible for some systems, and potentially infinite for others. To examine this question, it is useful to examine the system in terms of the actual particle volume per unit of vessel area, rather than in terms of the fluidization height. The differential relationship between a change in the specific volume of the particles, and the system volume is given by

$$dV_i = \phi_i dz \tag{31}$$

Incorporating Eq. 31 into Eq. 13 gives

$$\frac{d\phi_{ni}}{(\phi_{ni} + \beta_i)(1 - \phi_{ni})} = \frac{(\phi_{mi} - \phi_{mj})U_{ij}dV_i}{\phi_{mi}\alpha d_i} \tag{32}$$

Formation of partial fractions, and integration from $\phi_{ni} = \phi_{ni}$ to $\phi_{\mathrm{nio}}$, and $V_i = V_i$ to $V_{io}$ gives

$$\left(\frac{\phi_{nio} + \beta_i}{\phi_{ni} + \beta_i}\right)\left(\frac{1 - \phi_{ni}}{1 - \phi_{nio}}\right) = \exp\left(\frac{U_{ij}(V_{io} - V_i)}{\alpha d_i}\right) \tag{33}$$

Based on the exponential term in Eq. 33, the characteristic volume of the transition zone for species $i$ is

$$V_{Ti} = \frac{-\alpha d_i}{U_{ij}} \tag{34}$$

Similarly, for species $j$, the solution is

$$\left(\frac{\phi_{njo} + \beta_j}{\phi_{nj} + \beta_j}\right)\left(\frac{1 - \phi_{nj}}{1 - \phi_{njo}}\right) = \exp\left(\frac{-U_{ji}V_j)}{\alpha d_j}\right) \tag{35}$$

and the characteristic volume of the transition zone is

$$V_{Tj} = \frac{\alpha d_j}{U_{ji}} \tag{36}$$

Equations 34 and 36 indicate that the characteristic thickness of the transition zone for species $i$ and $j$, respectively, scales directly with the principal length scale of the system, the particle diameter, and inversely with the respective normalized segregation parameter. This result is sensible, and explains why the transition zone in some systems is much larger, typically, than in other systems. For example, a large segregation number corresponds to a sharp interface between the two species, while a very small segregation number indicates a large transition zone.

Figures 2 and 3 show the results obtained using two other binary systems in which the particles are again 1.0 to 1.18 mm in size. In Figure 2 the results produced were for particles having densities of 1,300 and 1,400 kg/m$^3$, whereas in Figure 3, the results are for particles having densities of 1,700 and 1,800 kg/m$^3$. The analysis was conducted using the Richardson and Zaki parameters for the respective monocomponent systems. These parameter values are shown in Table 1, and the superficial velocities are shown in Table 2. The curves through the data are based on Eq. 9, with $\alpha$ again equal to 0.7.

To obtain the level of agreement shown, however, it was necessary to adjust very slightly the values of the terminal velocities of the two species. The values of the terminal velocities required in order to achieve a satisfactory model fit of the concentration profile data, with $\alpha = 0.7$, are shown in Table 2. It is evident that, compared to the Richardson and Zaki based values in Table 1, the level of adjustment required was typically only 2%. In each case, the velocity of the denser species was decreased, while the velocity of the less dense species was increased. Given the existence of a particle-size range of 1.0 to 1.18 mm for each species, the need for these adjustments is entirely reasonable. However, it is useful to consider whether the adjustments can be justified in terms of apparent variations in the average particle sizes due to the effect of particle-size segregation.

Figure 4 shows the average particle sizes of the 1,700 and

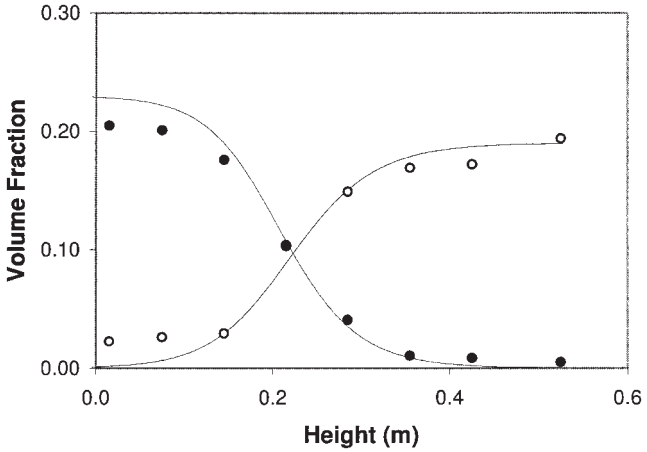


**Figure 2. Concentration profiles produced using particle species having densities of 1,300 and 1,400 kg/m$^3$ and diameters ranging from 1.0 to 1.18 mm, with the superficial velocity set at 0.0229 m/s.**

The curves through the data are based on Eqs. 17 and 23, with the dispersion coefficient, based on $\alpha = 0.7$ and $d = 0.00109$ m. Other parameter values, such as the monocomponent concentrations and segregation parameter values are derived from Table 2. Again, the open symbols and closed symbols denote the low and the high-density species, respectively.

1,800 kg/m$^3$ density species at different elevations. The open symbols denote the lower-density species, and the filled symbols the higher-density species. These data were obtained by analyzing the samples withdrawn at different elevations in the system, separating the two-particle species by hand, weighing each species, and then counting the numbers of particles. It was

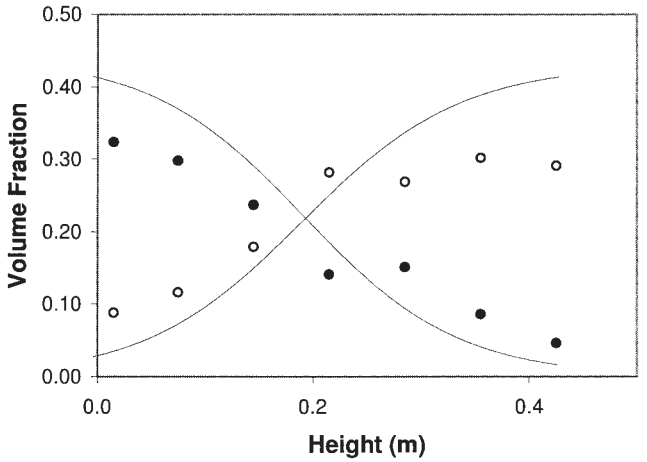


**Figure 3. Concentration profiles produced using particle species having densities of 1700 and 1800 kg/m$^3$ and diameters ranging from 1.0 to 1.18 mm, with the superficial velocity set at 0.0138 m/s.**

The curves through the data are based on Eqs. 17 and 23, with the dispersion coefficient, based on $\alpha = 0.7$ and $d = 0.00109$ m. Other parameter values, such as the monocomponent concentrations and segregation parameter values are derived from Table 2. Again, the open symbols and closed symbols denote the low and the high density species, respectively.

**Table 2. Additional Binary Fluidization Experiments**

| Particle Species (kg/m$^3$) | Adjusted Terminal Velocity (m/s) | Calculated Mono-Component Volume Fraction | Superficial Velocity (m/s) |
|---|---|---|---|
| 1300 | 0.047 | 0.19 | 0.0229 |
| 1400 | 0.051 | 0.23 | 0.0229 |
| 1700 | 0.081 | 0.43 | 0.0138 |
| 1800 | 0.083 | 0.44 | 0.0138 |

then possible to obtain the average mass of each particle present at a given elevation, for each of the two species. Then, assuming the particles were spheres, an average diameter was calculated.

There are some subtle issues concerning the data in Figure 4. The data in this Figure first indicates that particle-size segregation occurred in the fluidized bed. Second, the data in this Figure shows that at each level within the fluidized bed the average-particle size for the 1,700 kg/m$^3$ species is always larger than the average-particle size of the 1,800 kg/m$^3$ species. These data are, therefore, surprising given that the two species should have had virtually the same size distribution, both ranging nominally from 1.0 to 1.18 mm. Indeed, the particle species were prepared by subjecting particles covering a broader range of size to a separation over precise sieves of 1.0 and 1.18 mm.

However, a more careful consideration of the segregation indicates that the data are consistent with expectations. At the top of the fluidized bed, the concentration of the 1,800 kg/m$^3$ species is relatively low compared to the concentration of the 1,700 kg/m$^3$ species, as shown in Figure 3. The 1,800 kg/m$^3$ species present at the top of the bed will clearly be the very smallest of the 1,800 kg/m$^3$ species. The 1,700 kg/m$^3$ species present at the top of the bed will also consist of the very smallest of the 1,700 kg/m$^3$ species. However, given the much higher concentration of the 1,700 kg/m$^3$ species at this elevation, there will also be present some larger particles as well. Thus, the average particle size for the 1,700 kg/m$^3$ species will be greater than for the 1,800 kg/m$^3$ species. This argument also

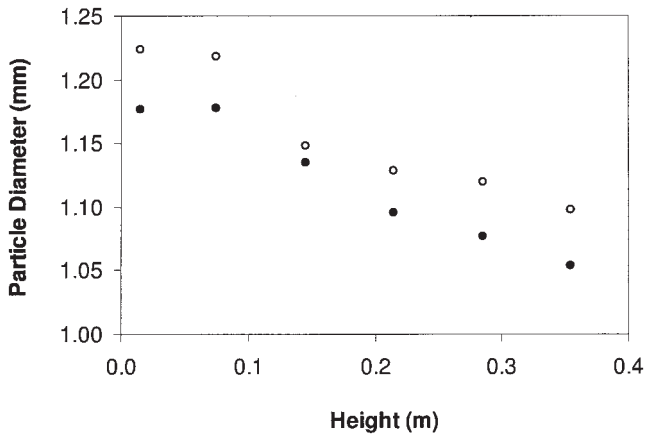


**Figure 4. Average-particle diameters for the 1,700 and 1,800 kg/m$^3$ species, based on the same conditions described in Figure 3.**

These data show the tendency for size segregation in this experiment. The open symbols denote the 1700 kg/m$^3$ species and the closed symbols the 1800 kg/m$^3$ species.

accounts for the data at the other elevations, including the data near the base of the fluidized bed. At the base, the concentration of the 1,700 kg/m$^3$ species is low, so only the very largest of the 1,700 kg/m$^3$ species will be present here. For the 1,800 kg/m$^3$ species, the concentration is much higher, and, hence, the very largest particles along with some smaller particles will be present. Thus, again, the average particle size for the 1,700 kg/m$^3$ species will be greater than for the 1,800 kg/m$^3$ species.

The average size of a given particle species in the fluidized bed can be calculated directly from the data in Figures 3 and 4. The weighted average diameter for species $i$ is

$$\overline{d}_i = \frac{\int_0^{h_{\max}} d_i \phi_i dh}{\int_0^{h_{\max}} \phi_i dh} \tag{37}$$

where $d_i$ is the average diameter at an elevation of $h$, $\phi_i$ the local-volume fraction at the same elevation, and $h_{max}$ the bed height. The average particle size for the 1,700 kg/m$^3$ species based on Eq. 37 was found to be 1.134 mm, and the average for the 1,800 kg/m$^3$ species 1.133 mm, almost the same even though the average size of each species at a given elevation in Figure 4 appears to differ by as much as 3.3% at virtually every location. It is noted that the small adjustments in the terminal velocities of the particle species to produce the theoretical curve in Figure 3 are consistent with the 3.3% difference in the average-particle diameter at a given location.

Equations 34 and 36 account for the size of the transition zone in the fluidized bed. The values of the segregation parameters $U_{ij}$ and $U_{ji}$, are, therefore, crucial. When the terminal velocities of the two species are very similar, these values approach a value of 0, and, hence, the transition zone becomes infinite in extent. Thus, the experiment involving particles species of density 1,700 and 1,800 kg/m$^3$ had the potential to produce significant relative errors in the values of $U_{ij}$ and $U_{ji}$. It is noted that the adjustment of the terminal velocities by typically 2% produced about a 50% reduction in the values of these segregation parameters. Conversely, a similar adjustment to the terminal velocities in the first set of experiments, involving particles of density 1,600 and 1,900 kg/m$^3$, would have had a negligible effect on the values of the segregation parameters. It is further noted that the role of the size segregation in the first set of experiments was substantially lower than in the latter experiments. Although it can be argued that the latter experiments are consistent with the general theory presented in this article, the generality of the expression for the dispersion coefficient is not proven in a definitive sense.

Further, it should be noted that the dispersion coefficients reported in virtually all previous studies are based on models that assume the dispersion coefficient is the same throughout the system. Here, the dispersion coefficient depends on the local conditions, and so varies appreciably throughout the system, as shown in Figure 5 for the conditions in Figure 1f. In the monocomponent zone of species $i$, the dispersion coefficients of the two species were the same, given they had the same particle size. Also, at any given location in the transition zone, the two species had the same dispersion coefficient. In

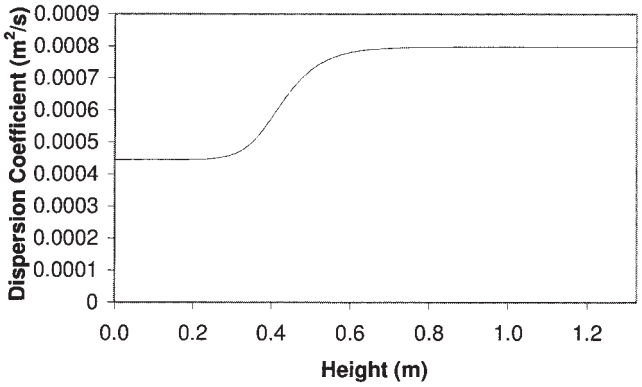


**Figure 5. Dispersion coefficient calculated using Eq. 9, with $\alpha$ = 0.7 and $d$ = 0.0019 m, based on the data in Figure 1f, and, hence, a superficial velocity of 0.058 m/s.**

It is evident that the dispersion coefficient varies significantly due to changes in the local volume fraction of solids.

moving vertically up through the system the volume fraction gradually decreased, while the superficial velocity was the same at all elevations. Hence, the dispersion coefficient varied inversely with the factor, $\phi(1-\phi)$, where $\phi$ is the total volume fraction of solids at a given location. The use of a local, and, hence, variable dispersion coefficient in this study makes accurate comparisons with previous data problematic.

The particle Reynolds number in this study was relatively high at 50 to 100, which suggests that the particle-particle interactions were more relevant than the particle-particle-fluid interactions in governing the dispersion. Although the particles have a notional velocity of zero relative to the vessel, they do exhibit significant random motion and, hence, collisions with neighbors, and, hence, an approach based on the kinetic theory of gases appears to apply. We note that a more complete analysis of the mean free path[7] leads to a result smaller than we obtained by a factor of $\sqrt{2}$. Thus, combining the correct mean free path, with the final result for the dispersion coefficient, the average particle velocity (root mean square speed) is $0.7x\sqrt{2}x6xU_f \sim 6U_f$. This quantity could in turn be used to arrive at a kinetic energy, and, hence, a granular temperature for the system.

Gidispow[7] has noted that the mean free path should not increase without bound as the volume fraction approaches zero, but rather become equal to the vessel diameter rather than exceed the vessel diameter. Hence, the dispersion coefficient should also remain finite. However, there should be no problem in the dispersion coefficient increasing to an infinite level as the volume fraction approaches zero. As the volume fraction approaches zero, the local concentration gradient should also approach a level of about zero given that the change in concentration over any finite length-scale should be close to zero. Assume that the local concentration gradient is given by $k\phi/d$ where $k$ is a scalar, $\phi$, the local concentration, and $d$ a relevant length-scale. As noted in the article the dispersion coefficient is $\alpha d U_f/\phi$. Hence, the dispersion flux, $Dd\phi/dz$ should be given by $(\alpha d U_f/\phi)(k\phi/d) = \alpha k U_f$. Thus, the dispersion flux will remain finite, limited in magnitude by the velocity term which, as noted earlier, is about $6U_f$.

## Conclusions

The liquid fluidization of a binary system of particles was investigated. The particles were nominally of the same size, with differences governed primarily by the particle density. A general expression for the dispersion coefficient was proposed, dependent on the particle diameter, the local volume fraction of the solids, and the local interstitial fluidization velocity. With one adjustable parameter, $\alpha$, fixed at a value of 0.7, it was possible to describe the concentration profiles of both species over a broad range of fluidization velocities. The remaining parameters were derived from the monocomponent descriptions, based on the Richardson and Zaki equation.[12] Additional binary systems that displayed a greater tendency to mix, were also tested. These experiments indicated that the model could be extended to a broader range of conditions. However, there was some uncertainty in the value of the segregation parameter in the transition zone between the monocomponent zones, because the terminal velocity values were so similar, and, hence, size segregation more significant.

## Literature Cited


1. Pruden BB, Epstein N. Stratification by size in particulate fluidization and in hindered settling. *Chem Eng Sci*. 1964;19:696-700.
2. Batchelor GK. A new theory of the stability of a uniform fluidized bed. *J of Fluid Mechanics*. 1988;193:75-110.
3. Davis RH, Hassen MA. Spreading of the interface at the top of a slightly polydisperse sedimenting suspension. *J of Fluid Mechanics*. 1988;196:107-34.
4. Dorgelo EAH, Van Der Meer AP, Wesselingh JA. Measurement of the axial dispersion of particles in a liquid fluidized bed applying random walk model. *Chem Eng Sci*. 1985;40(11):2105-2111.
5. Kang Y, Nah JB, Min BT, Kim SD. Dispersion and fluctuation of fluidized particles in a liquid-solid fluidized bed. *Chem Eng Comm*. 1990;97:197.
6. Asif M, Petersen JN. Particle dispersion in a binary solid-liquid fluidized bed. *AIChE J*. 1993;39(9):1465-1471.
7. Gidaspow D. *Multiphase flow and fluidization: Continuum and kinetic theory descriptions*. San Diego, CA: Academic Press; 1994.
8. Kennedy SC, Bretton RH. Axial dispersion of spheres fluidized with liquids. *AIChE J*. 1966;12**:**24**.**
9. Lockett MJ, Al-Habbooby HM. Differential settling by size of two particle species in a liquid. *Trans of the Inst of Chem Eng*. 1973;51: 281-292.
10. Callen AM, Pratten SJ, Lambert N, Galvin KP. Measurement of the Density Distribution of a System of Particles using Water Fluidization. *4th World Congress on Particle Technology*. Sydney. 2002;Paper 275.
11. Ramirez WF, Galvin KP. Dynamic model of multispecies segregation and dispersion in liquid fluidized beds. *AIChE J*. 2005;51(7):2103-2108.
12. Richardson JF, Zaki WN. The sedimentation of a suspension of uniform spheres under conditions of viscous flow. *Chem Eng Sci*. 1954; 3:65-73.
13. Tory, EM. personal communication, 2006.
14. Bargiel M, Tory EM. Simulation of sedimentation and fluidization of polydisperse suspension via a Markov model. *Chem Eng Sci.* 2006; 61(17):5575–5589.


*Manuscript received Feb. 26, 2006, and revision received Jun. 2, 2006.*